Life Sciences 231 (2019) 116674

Contents lists available at ScienceDirect

Life Sciences

journal homepage: www.elsevier.com/locate/lifescie

Endogenous peptide LYENRL prevents the activation of hypertrophic scar-derived fibroblasts by inhibiting the TGF-β1/Smad pathway

Xiaojun Ji[a], Zhe Tang[b], Weiwei Shuai[b], Zhirui Zhang[a], Jingyun Li[c], Ling Chen[d], Jing Cao[b,*], Wu Yin[a,*]

[a] State Key Lab of Pharmaceutical Biotechnology, College of Life Sciences, Nanjing University, Nanjing 210046, China
[b] Department of Pharmacy, Women's Hospital of Nanjing Medical University (Nanjing Maternity and Child Health Care Hospital), Nanjing 210004, China
[c] Nanjing Maternal and Child Health Medical Institute, Women's Hospital of Nanjing Medical University (Nanjing Maternity and Child Health Care Hospital), Nanjing 210004, China
[d] Department of Plastic & Cosmetic Surgery, Women's Hospital of Nanjing Medical University (Nanjing Maternity and Child Health Care Hospital), Nanjing 210004, China

ARTICLE INFO

Keywords:
Endogenous peptide
LYENRL
Hypertrophic scars
TGF-β1/Smad
Fibroblasts

ABSTRACT

Hypertrophic scar formation is a fibroproliferative disorder caused by abnormal wound healing. At present, there are limited treatment strategies for hypertrophic scars. In this study, we identified an endogenous peptide, LYENRL, through peptidomics screening that is downregulated in scar skin tissues. The peptide exhibited concentration dependent inhibitory effects on the proliferation, migration and extracellular matrix (ECM) production of scar fibroblasts. By eukaryotic transcriptome sequencing analysis, we noted that LYENRL downregulated gene sets in scar fibroblasts were associated with the transforming growth factor-β (TGF-β) signaling pathway. Further experiments revealed that LYENRL was able to inhibit the activation of TGF-β1/Smad signaling and TGF-β1-induced activation of scar fibroblasts at the source by blocking the binding of AP-1 to the corresponding region of the *Tgfb1* promoter, which in turn inhibited gene expression of *Tgfb1*. Taken together, we concluded that the effects of LYENRL on scar fibroblasts make it a potential peptide drug for hypertrophic scar treatment.

1. Introduction

Hypertrophic scar is a fibrotic proliferative tissue formed after deep skin trauma, and its incidence rate is as high as 70% [1,2]. Hypertrophic scar formation is characterized by the abnormal proliferation of fibroblasts and excessive collagen deposition. A wide range of hypertrophic scars leads to muscle contracture and limited movement, considerably decreasing patient quality of life. Currently, pressure therapy, surgical resection and corticosteroid injection are the main methods used to treat hypertrophic scars; however, limitations or adverse reactions exist in these treatments [3]. Therefore, identifying new strategies for hypertrophic scar treatment has become a hot spot for research in the field of wound healing in recent years.

Peptidomics is an emerging branch of proteomics widely used in studies of food digestion, identification of disease biomarker and discovery of new functions for endogenous peptides [4]. To date, peptidomics is primarily used in disease biomarker screening. A variety of peptide biomarkers have been identified by peptidomics, such as β-amyloid 1-42 and tau for Alzheimer's disease prediction [5], and urinary peptides for acute and chronic kidney diseases [6–8], prostate cancer [9] and coronary artery diseases [10]. In addition to being biomarkers, certain endogenous peptides are biologically active. For example, neuropeptide is an endogenous peptide that acts as a neurotransmitter, neurohormone, and neuromodulator [11]. In addition, many hormones are also endogenous peptides including insulin, prolactin and oxytocin. Studies have also shown the antinociception effect of the endogenous peptide MERF, protection against cardiomyocyte ischemic injury by apelin and the immunomodulatory effects of bursopentin [12–14].

Abbreviations: ActD, Actinomycin D; AP-1, Transcription factor AP-1; ChIP, Chromatin immunoprecipitation; ECM, Extracellular matrix; Egr1,, Early growth response 1; GO, Gene ontology; HSF, Human scar fibroblast; KEGG, Kyoto encyclopedia of genes and genomes pathway; LC-MS/MS, Liquid chromatography-tandem mass spectrometry; SBE, Smad binding elements; TGF-β1, Transforming growth factor beta 1; TLR2, Toll like receptor 2; VEGF, Vascular epidermal growth factor

* Corresponding authors at: College of Life Sciences in Nanjing University (Xianlin Campus), Lab of Biochemical and Molecular Pharmacology, State Key Lab of Pharmaceutical Biotechnology, 168# Xianlin Ave, Qixia District, Nanjing 210046, China; Department of Pharmacy, Women's Hospital of Nanjing Medical University (Nanjing Maternity and Child Health Care Hospital), 123# Tianfei Street, Mochou Road, Qinhuai District, Nanjing 210004, China.
E-mail addresses: njfycj@163.com (J. Cao), wyin@nju.edu.cn (W. Yin).

https://doi.org/10.1016/j.lfs.2019.116674
Received 10 May 2019; Received in revised form 19 July 2019; Accepted 19 July 2019
Available online 22 July 2019

However, endogenous peptides for the treatment of hypertrophic scars have yet to be identified.

In our previous study, we performed a comparative peptidomics analysis of human hypertrophic scar tissue and matched normal skin using liquid chromatography-tandem mass spectrometry (LC-MS/MS). A total of 179 differentially expressed peptides were identified in human hypertrophic scar skin tissues compared with matched normal skin tissues. Gene ontology (GO) and Kyoto Encyclopedia of Genes and Genomes pathway (KEGG) analyses revealed that the precursor proteins of these differentially expressed peptides were associated with cellular processes, biological regulation, binding and structural molecule activity ribosome and PPAR signaling pathway, etc. [15]. This study is a continuation of our previous study, which intends to further analyze these differentially expressed peptides for the purpose of identifying endogenous peptides involved in hypertrophic scar formation.

2. Materials and methods

2.1. Reagents

Peptides LYENRL, ASGVA, FITC-labeled LYENRL (FITC-LYENRL) and FITC-labeled EHTYGQAGSQHEEPEFTVHER (FITC-EHTYG) were chemically synthesized by a biological company (Abclonal, Wuhan, China). TGF-β1 (100-21) was purchased from Peprotech (Rocky Hill, CT, USA). Actinomycin D (ActD, HY-17559) was obtained from MedChemExpress (NJ, USA). Polyjet (SL100688) and Lipofectamine 2000 (11668-019) transfection reagents were purchased from SignaGen (Gaithersburg, MD, USA) and Invitrogen (Grand Island, NY, USA), respectively.

2.2. Clinical sample collection and peptide identification

Hypertrophic scar tissues and paired normal skin tissues were obtained from 6 different patients admitted to the Women's Hospital of Nanjing Medical University for scar removal. This study was approved by the Medical Ethics Committee of the Women's Hospital of Nanjing Medical University (No. [2013]48 and No. [2014]95). The methods for collecting patient information and performing peptide extraction and peptide identification using LC-MS/MS were previously described [15]. This research was carried out in accordance with the World Medical Association Declaration of Helsinki, and all subjects provided written informed consent.

2.3. Cell culture and treatment

The human hypertrophic scar fibroblast (HSF) cell line was obtained from Nuopuxin Biotechnology Co., Ltd. (Nanjing, China). The normal human dermal fibroblast (BJ) cell line used in this study was obtained from the American Type Culture Collection (ATCC, Manassas, VA, USA). The cells were cultured in DMEM (319-005-CL, Wisent, Nanjing, China), supplemented with ascorbic acid phosphate (2.5 mg/L) (49752, Sigma-Aldrich, St. Louis, MO, USA), penicillin (100 U/mL), streptomycin (100 μg/mL) (450-201-EL, Wisent, Nanjing, China) and fetal bovine serum (10% in HSF cell culture and 15% in BJ cell culture) (30084.03, Hyclone, Logan, UT, USA), and were maintained in a humidified incubator (37 °C and 5% CO_2). The cells were passaged when confluence reached 70%. Cells passaged for > 20 passages were not used for subsequent experiments. BJ cells and HSF cells were serum starved for 12 h prior to treatment, followed by treatment with drugs or peptides in the absence of serum. The peptides used in this study were dissolved in sterile water to 1, 10, 20, 50 and 100 mM, respectively, and then added to the cell culture medium at a ratio of 1:1000 (v/v). The cells were harvested for subsequent experiments after treatment for various time points.

2.4. Bioinformatics analysis of peptides

Using molecular weight, isoelectric point, instability index, aliphatic index and grand average of hydropathicity (GRAVY) index, each peptide were identified using the ProtParam tool provided by Expasy Bioinformatics Resource Portal (http://web.expasy.org/protparam). Homology alignment of the same peptide and its precursor protein originating from different species was accomplished using the UniProt website (http://www.uniprot.org).

2.5. Eukaryotic transcriptome sequencing

Total RNA was extracted from treated cells using TRIzol reagent (15596026, Invitrogen, Carlsbad, CA, USA) according to the manufacturer's instructions. RNA samples were subsequently subjected to quality inspection, including purity, concentration, integrity and RIN value detection of RNA by a company (Majorbio, Shanghai, China). Subsequently, RNA samples were submitted for eukaryotic transcriptome sequencing, and the sequencing data were obtained and compared with the reference sequence. Gene sets were established after differential analysis of gene expression. GO function enrichment analysis and signal pathways KEGG enrichment analysis were performed on these gene sets. All data analyses were performed on the I-Sanger Bioinformatics Cloud Platform (https://www.i-sanger.com).

2.6. CCK-8 and EdU tests

To test the effects of peptides or TGF-β1 on cell viability, HSF cells were cultured in 96-well microplates at a density of 5000 cells per well. After treatment, CCK-8 solution (C0042, Beyotime, Nantong, China) was added into each well (10 μL CCK-8/100 μL culture medium) and incubated at 37 °C for 2 h. The absorbance of each well was determined by a microplate reader at a measurement wavelength of 450 nm and a reference wavelength of 620 nm. Cell proliferation was measured using an EdU kit (C0085S, Beyotime, Nantong, China). HSF cells were cultured in 6-well plates at a density of 20×10^4 cells per well. Assays were performed according to the manufacturer's instructions. The experiments were repeated 3 times, and the ratio of the treatment group to the control group was used for statistical comparisons.

2.7. Hydroxyproline content measurement

Levels of hydroxyproline in cells were detected using a commercial kit (A030-1-1, Jiancheng Bioengineering Institute, Nanjing, China). The oxidation product produced by hydroxyproline under the action of oxidants exhibits a purple-red color in the action of dimethylaminobenzaldehyde, and its content can be calculated according to OD values measured at 550 nm [16].

2.8. Western blotting

The culture medium of the BJ or HSF cells (cultured in 6-well plates) was discarded after treatment, and cells were washed with PBS (cooled before use) three times, followed by the addition of RIPA lysis buffer (containing cocktail inhibitor). Then, cells were collected into a centrifuge tube and lysed on ice for 30 min. The supernatant was obtained by centrifugation, and the protein concentration was determined by a BCA protein assay kit (P0010, Beyotime, Nantong, China). Proteins were subjected to SDS-PAGE and transferred to PVDF membranes. Subsequently, membranes were incubated with specific primary antibodies at 4 °C overnight. Antibodies against p-Smad2 (ab53100, Ser467, 1:1000), p-Smad3 (ab52903, Ser423/425, 1:1000) and Smad2/3 (ab202445, 1:1000) were purchased from Abcam (Cambridge, UK). Gapdh (AP0063, 1:5000) antibody was obtained from Bioworld Technology (Nanjing, China). The next day, membranes were washed with PBST and incubated with a HRP-labeled secondary antibody

Table 1
Primers used in RT-PCR, plasmid construction and ChIP analysis.

Primer name	Forward primer (5′-3′)	Reverse primer (5′-3′)	Product length (bp)
Col1a1-human	GCAAGGTGTTGTGCGATGACG	AGGGAGACCACGAGGACCAGAG	374
Col1a2-human	ATGCCTAGCAACATGCCAATC	CAGCAAAGTTCCCACCGAGA	185
Col3a1-human	GCTCTGCTTCATCCCACTATTA	TGCGAGTCCTCCTACTGCTAC	471
Acta2-human	CGGGACATCAAGGAGAAACT	AATGCCAGGGTACATAGTGG	300
Fn1-human	GCCAACCTTTACAGACCTATCC	GGTGGTGAAGTCAAAGCGAGT	302
Tgfb1-human	CTAATGGTGGAAACCCACAACG	TATCGCCAGGAATTGTTGCTG	209
Egr1-human	GAGCGATGAACGCAAGAGGCA	GGATGGGTATGAGGTGGTGGC	184
Jun-human	TGGAAACGACCTTCTATGACGA	ATGTGCCCGTTGCTGGACTG	250
Fos-human	GTCTCCAGTGCCAACTTCATTC	GCAGCCATCTTATTCCTTTCC	290
pTgfb1-1362	TTTGGTACCGGATCCTTAGCAGGGGAGTAAC	GGAAGATCTCGGAGGGAGGTGGGAGGGAGAT	1372
pTgfb1-974	TTTGGTACCACGGGCTTTCGTGGGTGGTGGG	GGAAGATCTCGGAGGGAGGTGGGAGGGAGAT	984
pTgfb1-618	TTTGGTACCTGTATGGGGTCGCAGGGTGTTG	GGAAGATCTCGGAGGGAGGTGGGAGGGAGAT	628
pTgfb1-386	TTTGGTACCGGTCGGCTCCCCTGTGTCTCAT	GGAAGATCTCGGAGGGAGGTGGGAGGGAGAT	396
pTgfb1-74	TTTGGTACCGCTTCAAAACCCCCTGCCGACC	GGAAGATCTCGGAGGGAGGTGGGAGGGAGAT	84
Tgfb1-human for ChIP	CCCTTCCATCCTTCAGGTGTCC	CAGAACGGAAGGAGAGTCAGGC	120

(BS13278, 1:50000, Bioworld, Nanjing, China). The luminescent substrate was added and autoradiographed, and protein expression was determined based on the exposure bands. Intensity of the images was analyzed using ImageJ software [17].

2.9. RNA isolation and RT-PCR

Total RNA was isolated from the BJ or HSF cells using TRIzol reagent according to the manufacturer's instructions. cDNA was synthesized using 1 μg RNA and reverse transcribed using a First Strand cDNA Synthesis Kit (11123ES10, Yeasen, Shanghai, China). PCR was carried out for 28 cycles by denaturing at 94 °C for 30 s, annealing at 52–58 °C for 30 s, and extension at 72 °C for 5 min. Then, PCR products were separated on 1% agarose gels, stained with GelRed (D0140, Beyotime, Nantong, China) and visualized under ultraviolet light. Image intensity was analyzed using ImageJ software. Primers were synthesized at Tsingke (Nanjing, China) (Table 1).

2.10. Collagen 1α1 and TGF-β1 content measurement

Levels of collagen 1α1 (SEKH-0401) and TGF-β1 (SEKH-0316) in cell culture medium were measured by enzyme-linked immunosorbent assay (Solarbio, Beijing, China). Briefly, after the sequential addition of standards or cell culture medium to monoclonal antibody coated microwells, HRP-labeled specific antibody was added to wells to form an antibody-antigen-enzyme-labeled antibody complex. The substrate TMB was then added and converted to blue under the catalysis of the HRP enzyme and turned into the final yellow color by the addition of acid. Color gradation was positively correlated with antigen content in the sample. Absorbance (OD value) was measured at 450 nm using a microplate reader, and the antigen concentration was calculated according to the standard curve.

2.11. Scratch test

Cells were seeded into 6-well plates and cultured in an incubator. A pipet tip (0–200 μL) was used to draw a straight line along the ruler in the middle of the 6-well plate, keeping the tip perpendicular, when cell density was approximately 70–80%. Then, the cells were gently washed with sterile PBS 3 times to remove the scoring cells. The medium was re-added, the cells were treated with TGF-β1 or peptides and the cells were subsequently imaged at 0 h, 12 h, 24 h and 36 h. Scratch areas and wound healing percentages were calculated using ImageJ software (Version 1.52a, NIH, USA).

2.12. Transwell test

The cells were serum starved for 12 h to remove the effect of serum before the formal experiment. Then, the cells were routinely digested, centrifuged, washed with PBS and resuspended in serum free medium. Then, the cell density was adjusted to 1×10^5/mL, and the cell suspensions (100 μL) were added to transwell chambers (3378, Corning, NY, USA). Then, 500 μL fetal bovine serum containing medium was added to the lower chamber of the 24-well plate. The cells were treated with TGF-β1 or peptides for 24 h, after which the chamber was removed, washed with PBS 3 times, fixed with 95% ethanol for 5 min and stained with crystal violet solution (4 mg/mL) for 5 min. The cells in the inner layer of the chamber were carefully wiped with a cotton swab, and cells that had migrated to the outer layer of the chamber were counted under an inverted microscope (Olympus, Tokyo, Japan).

2.13. Dual luciferase reporter assay

Renilla luciferase and pGL3-Basic firefly luciferase constructs were obtained from Promega (Madison, WI, USA). To generate a construct containing the human *Tgfb1* promoter and its deletion mutants, promoter sequences of human *Tgfb1* were amplified from HSF genomic DNA using FastPfu DNA polymerase (AP221, TransGen Biotech, Beijing, China). DNA fragments were purified and cloned into the pGL3-Basic luciferase reporter construct using *Kpn*I and *Bgl*II. The primer sequences are shown in Table 1. Point mutations in the Egr1 and AP-1 sites were generated by a two-step PCR method. HSF cells were transiently transfected with the indicated constructs (0.8 μg) and pRL-TK (0.08 μg) for 24 h using a PolyJet DNA transfection reagent according to the manufacturer's instruction. Then, the cells were treated with peptides for another 12 h. For luciferase assays, HSF cells were harvested and lysed in lysis buffer. Promoter activities were measured using a Dual Luciferase Reporter Assay System (E1910, Promega, Madison, WI, USA) according to the manufacturer's instruction. The ratio of firefly luciferase to renilla luciferase was regarded as the activity of the promoter.

2.14. Chromatin immunoprecipitation

Chromatin immunoprecipitation was performed as previously described [18]. c-Jun (9165), c-Fos (2250) and Egr1 (4154) antibodies were obtained from Cell Signaling Technology (Beverly, MA, USA). The primer sequences are shown in Table 1.

2.15. Peptide distribution detection and Smad activity measurement

To detect the distribution of peptides in cells, HSF cells were treated

with unlabeled or FITC-labeled peptides for 12 h, then the cells were fixed with 4% paraformaldehyde for 30 min at room temperature. After three extensive washings with PBS, the cells were stained with DAPI (C1005, Beyotime, Nantong, China) for 5 min to detect the cell nuclei. The fluorescence images were viewed with a confocal microscope (TCS SP8-MaiTai M, Leica, Wetzlar, Germany). All of the above operations were carried out in the dark. For Smad activity measurement, HSF cells were previously transfected with EGFP-Smad reporter plasmids (11743ES03, Yeasen, Shanghai, China) for 24 h, then the cells were treated with TGF-β1 and different concentrations of LYENRL. After treatment, the cells were fixed with 4% paraformaldehyde and stained with DAPI. Fluorescence microscopy (NE900, Nexcope, Ningbo, China) was utilized to view the images.

2.16. Statistical analysis

The data are presented as the mean ± SD. Statistical analysis was performed using SPSS statistical software (Version 24.0). For multiple comparisons, one-way analysis of variance (ANOVA) was applied, followed by LSD post hoc analysis for data meeting homogeneity of variance or by Dunnett's T3 analysis for data without equal variances. GraphPad Prism software (Version 5) was utilized to create graphs. In all cases, differences were considered significant at $P < 0.05$.

3. Results

3.1. Identification of differentially expressed peptides in hypertrophic scar tissues

In our previous study, endogenous peptides in hypertrophic scar tissues and matched normal skin tissues were detected using LC-MS/MS and 1697 peptides were identified. Among these peptides, 78 peptides were highly expressed in normal skin tissues and were not expressed in corresponding hypertrophic scar tissues (Fig. 1A). The lengths of these endogenous peptides ranged from 6 to 25 amino acids, among which the majority were concentrated between 11 and 14 amino acids (Fig. 1B). In addition, the molecular weight of these endogenous peptides was distributed between 800 and 2600 Da, and the isoelectric points were distributed between 3.0 and 11.0 (Fig. 1C and D).

By bioinformatics comparison, these 78 endogenous peptides were shown to derive from 31 precursor proteins (Table 2). To verify the biological functions of these peptides at the cellular level, we screened peptides with high stability (instability < 0) and fat solubility (aliphatic index > 100) to ensure that the selected peptides function well in the cells. According to the filter conditions stated above, six peptides derived from three precursor proteins of hemoglobin subunit α, cofilin-1 and leucine-rich repeat-containing protein 15 (LRRC15) were selected (Table 3). Considering that hypertrophic scar tissue lack blood vessels, endogenous peptides derived from hemoglobin reduction in hypertrophic scar tissue were expected. Thus, these peptides were temporarily excluded from subsequent analysis. As a result, the remaining two endogenous peptides, LYENRL and ASGVAVSDGVIKV (ASGVA), were selected for the further assessment of biological function in this study.

3.2. The endogenous peptide LYENRL inhibits scar hyperplasia in vitro

What are the effects of these reduced peptides on hypertrophic scars? As abnormal fibroblast proliferation and excessive collagen deposition are important characteristics of hypertrophic scar formation [19], we tested the effects of the two abovementioned selected peptides on fibroblast proliferation and collagen deposition in subsequent experiments. Chemically synthesized peptides, LYENRL and ASGVA, were applied to human hypertrophic scar fibroblasts (HSF) for 24 h, and the results revealed that LYENRL inhibited the proliferation of HSF cells at a dose of 50 μM, whereas ASGVA had no significant effect on proliferation of HSF cells at this dose (Fig. 2A). Hydroxyproline is a specific amino acid in collagen whose content reflects collagen content [20]. In this study, LYENRL exhibited a strong inhibitory effect on hydroxyproline content in HSF cells, while the effect of ASGVA was weak (Fig. 2B). In addition, LYENRL inhibited gene expression of type I and type III collagen in HSF cells. In contrast, ASGVA showed little effect on the expression of these genes (Fig. 2C). Taken together, we believed that LYENRL may have an inhibitory effect on hypertrophic scar formation, whereas ASGVA may not have this potential. Bioinformatics analysis demonstrated that LYENRL is highly conserved in LRRC15 originating from human, mouse, rabbit, bovine, horse and rhesus species (Fig. 2D). Moreover, FITC-labeled LYENRL peptide can not only enter the cytoplasm, but also enter the nucleus of HSF cells. To exclude non-specific binding, we labeled a hydrophilic peptide with an amino acid sequence of EHTYGQAGSQHEEPEFTVHER (EHTYG) that downregulated in hypertrophic scar tissues using FITC. The results showed that this peptide can enter the cytoplasm of some cells, but it cannot enter into the nuclei. (Fig. 2E).

To further verify the role of LYENRL in hypertrophic scar formation, the effects of different concentrations of LYENRL on hypertrophic scar formation at different time points were measured. The CCK-8 assay demonstrated that 10 μM LYENRL exhibited an inhibitory effect on the viability in HSF cells at 24 h, which occurred in a concentration dependent manner. However, increasing the incubation time to 48 h did not enhance the inhibitory effect of this peptide on the viability of HSF cells (Fig. S1A). In accordance with the above results, LYENRL inhibited the proliferation of HSF cells, and the inhibitory effect was dose dependent (Fig. 3A). Hydroxyproline content and type I collagen secretion were elevated, and LYENRL reduced hydroxyproline content at doses of 10 μM, 20 μM, 50 μM and 100 μM in HSF cells, as well as the level of type I collagen secretion (Fig. 3B and C). The effects of LYENRL on the expression of collagen and fibrosis-related genes in HSF cells were examined by PCR, and fibroblasts from human normal skin (BJ cells) were used as controls. Compared with BJ cells, the expression of type I and type III collagen, *Acta2* and *Fn1* was significantly upregulated in HSF cells. Nevertheless, LYENRL inhibited expression of these genes in a dose dependent manner, with no obvious significant differences between 24 h and 48 h (Fig. 3D and E). In addition, a scratch test was performed to observe the effect of LYENRL on migration in HSF cells. A low concentration of LYENRL (1 μM) started to slow the healing rate of scratches, and this effect began to become significant when the peptide concentration increased to 10 μM. In addition, the greater the concentration was, the more pronounced the inhibitory effect was (Figs. 3F, G and S1B). However, LYENRL did not show similar effects on BJ cells. Treatment with LYENRL at doses ranging from 1 to 100 μM for 24 h or 48 h had no effect on hydroxyproline content and collagen 1α1 secretion (Fig. S1C and D). Moreover, these concentrations of LYENRL did not inhibit the expression of fibrosis-related genes in BJ cells (Fig. S1E and F).

Combined with the above results, we concluded that LYENRL inhibited the proliferation and migration of human hypertrophic scar fibroblasts and reduced the synthesis and secretion of collagen, resulting in inhibition of scar hyperplasia.

3.3. Transcriptome sequencing analysis of LYENRL in HSF cells

To investigate the underlying mechanism of LYENRL-induced inhibition of scar hyperplasia, transcriptome sequencing analysis was performed to detect differentially expressed genes in HSF cells after treatment with LYENRL. The results revealed that 329 genes were upregulated by LYENRL (fold > 2, $p < 0.05$) (Fig. 4A). GO analysis showed that the 304 downregulated genes participated in the regulation of proteinaceous extracellular matrix, extracellular matrix, extracellular matrix organization, extracellular structure organization and angiogenesis (Fig. 4B). Among these genes, the majority were related to the formation of hypertrophic scars and the process of fibrosis. Meanwhile, the genes downregulated by LYENRL were associated with

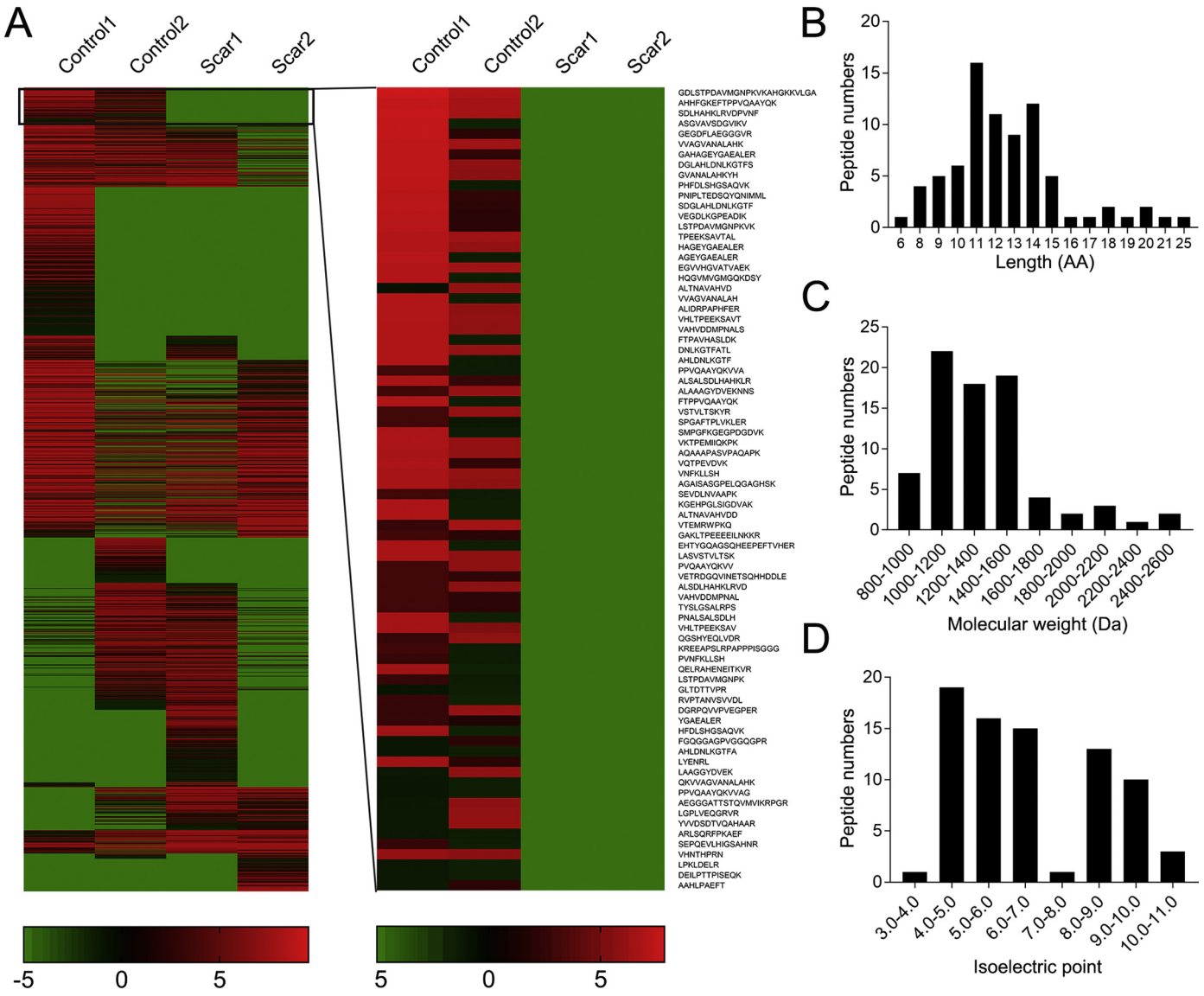

Fig. 1. Identification of differentially expressed endogenous peptides in hypertrophic scar tissues. (A) Hierarchical clustering of differentially expressed peptides. Clustering of all differentially expressed endogenous peptides in scar tissues and surrounding normal skin tissues (left). Clustering of endogenous peptides that not existed in scar tissues (right). Control: normal skin tissues; scar: hypertrophic tissues. (B) Length of the endogenous peptides that not existed in scar tissues. (C) Molecular weight of the endogenous peptides that not expressed in scar tissues. (D) Isoelectric point distribution of the endogenous peptides that not expressed in scar tissues.

protein digestion and absorption, AGE-RAGE, Hippo, TGF-β and ECM-receptor interaction signaling pathways, as shown by KEGG analysis (Fig. 4C). In these pathways, the TGF-β signaling pathway is undoubtedly one of the most widely studied pathways, which is closely related to hypertrophic scar formation. Therefore, we focused on the role of LYENRL in TGF-β signaling in subsequent experiments.

To clarify the relationship between LYENRL and the TGF-β signaling pathway, genes related to the TGF-β pathway were examined. We found that *Tgfb1* and TGF-β signaling pathway target genes *Cdkn2b*, *Gdf1*, *Gdf6*, *Inhbe*, *Lefty2* and *Rhoa* were downregulated in response to LYENRL; however, *Tgif* and *Smads* were not influenced (Table 4). Therefore, we hypothesized that LYENRL likely inhibits the TGF-β1/Smad signaling pathway by decreasing *Tgfb1* gene expression. In addition, sequencing results showed that LYENRL downregulated the gene expression of type I, type III, type IV and type V collagens, among which type I collagen was the most obvious. Meanwhile, the fibrosis related genes *Acta2*, *Ctgf* and *Fn1* were also downregulated by LYENRL treatment in HSF cells (Table 5).

3.4. LYENRL inhibits TGF-β1-induced scar hyperplasia in vitro

We further validated the effect of LYENRL on TGF-β1 signaling at the cellular level. LYENRL decreased gene expression of *Tgfb1* in HSF cells by approximately 40%, 50% and 60% at concentrations of 10, 20 and 50 μM, respectively (Fig. 5A and B). At the same time, LYENRL exhibited an inhibitory effect on TGF-β1 secretion in HSF cells (Fig. 5C). Phosphorylation of Smad2/3 is an important feature of TGF-β1 signaling pathway activation, and LYENRL reduced the phosphorylation of Smad2 and Smad3 in HSF cells in a dose-dependent manner (Fig. 5D). In addition to inhibiting baseline TGF-β1/Smad signaling, LYENRL exerted inhibitory effects on TGF-β1-induced activation of this signaling pathway (Fig. 5E). After phosphorylation, Smad2 and Smad3 form a complex with Smad4, and subsequently, the Smad2/3/4 complex enters the nucleus and exerts transcriptional activation of target genes. In this study, we used a Smad-EGFP reporter plasmid to mimic the activation effect of Smads on target genes. Smads were partially activated to basal levels in HSF cells, whereas TGF-β1 significantly

Table 2
Endogenous peptides highly expressed in normal skin tissues and not expressed in the corresponding hypertrophic scar tissues. Sequence, length, mass, precursor protein, instability index and aliphatic index are presented.

Sequence	Length	Mass	Precursor protein	Instability index	Aliphatic index
VNFKLLSH	8	957.14	Hemoglobin subunit alpha	−39.44	133.75
YGAEALER	8	907.98	Hemoglobin subunit alpha	−12.48	73.75
AAHLPAEFT	9	956.07	Hemoglobin subunit alpha	42.26	76.67
PVNFKLLSH	9	1054.26	Hemoglobin subunit alpha	−12.54	118.89
ALTNAVAHVD	10	1010.11	Hemoglobin subunit alpha	−29.55	127
DNLKGTFATL	10	1079.22	Hemoglobin subunit alpha	−4.13	88
VSTVLTSKYR	10	1153.34	Hemoglobin subunit alpha	−7.91	97
AGEYGAEALER	11	1165.22	Hemoglobin subunit alpha	−13.2	62.73
ALTNAVAHVDD	11	1125.2	Hemoglobin subunit alpha	−25.95	115.45
FTPAVHASLDK	11	1185.35	Hemoglobin subunit alpha	18.88	80
LASVSTVLTSK	11	1105.3	Hemoglobin subunit alpha	9.09	132.73
PNALSALSDLH	11	1137.26	Hemoglobin subunit alpha	9.09	124.55
VAHVDDMPNAL	11	1181.33	Hemoglobin subunit alpha	27.65	106.36
HAGEYGAEALER	12	1302.37	Hemoglobin subunit alpha	−11.27	57.5
HFDLSHGSAQVK	12	1325.45	Hemoglobin subunit alpha	−6.52	65
LSTPDAVMGNPK	12	1229.41	Hemoglobin subunit alpha	−6.59	65
VAHVDDMPNALS	12	1268.41	Hemoglobin subunit alpha	26.18	97.5
ALSDLHAHKLRVD	13	1474.68	Hemoglobin subunit alpha	17.64	127.69
PHFDLSHGSAQVK	13	1422.56	Hemoglobin subunit alpha	−5.25	60
ALSALSDLHAHKLR	14	1531.78	Hemoglobin subunit alpha	27.83	132.86
GAHAGEYGAEALER	14	1430.5	Hemoglobin subunit alpha	−20.36	56.43
SDLHAHKLRVDPVNF	15	1747.97	Hemoglobin subunit alpha	19.44	97.33
AHLDNLKGTF	10	1115.25	Hemoglobin subunit beta	−12.62	88
PVQAAYQKVV	10	1102.3	Hemoglobin subunit beta	19.77	107
AHLDNLKGTFA	11	1186.33	Hemoglobin subunit beta	−10.56	89.09
FTPPVQAAYQK	11	1249.43	Hemoglobin subunit beta	44.11	44.55
GVANALAHKYH	11	1180.33	Hemoglobin subunit beta	34.12	89.09
TPEEKSAVTAL	11	1145.28	Hemoglobin subunit beta	46.81	80
VHLTPEEKSAV	11	1209.36	Hemoglobin subunit beta	54.53	97.27
VVAGVANALAH	11	1021.18	Hemoglobin subunit beta	1.37	150.91
PPVQAAYQKVVA	12	1270.49	Hemoglobin subunit beta	34.19	97.5
VHLTPEEKSAVT	12	1310.47	Hemoglobin subunit beta	43.74	89.17
VVAGVANALAHK	12	1149.36	Hemoglobin subunit beta	21.82	138.33
PPVQAAYQKVVAG	13	1327.55	Hemoglobin subunit beta	32.33	90
LSTPDAVMGNPKVK	14	1456.72	Hemoglobin subunit beta	−12.34	76.43
QKVVAGVANALAHK	14	1405.66	Hemoglobin subunit beta	14.07	118.57
SDGLAHLDNLKGTF	14	1487.63	Hemoglobin subunit beta	−6.16	90.71
AHHFGKEFTPPVQAAYQK	18	2056.31	Hemoglobin subunit beta	15.65	32.78
GDLSTPDAVMGNPKVKAHGKKVLGA	25	2490.9	Hemoglobin subunit beta	−20.24	78
VQTPEVDVK	9	1014.14	Neuroblast differentiation-associated protein AHNAK	8.3	96.67
SEVDLNVAAPK	11	1142.27	Neuroblast differentiation-associated protein AHNAK	30.45	106.36
VKTPEMIIQKPK	12	1411.77	Neuroblast differentiation-associated protein AHNAK	14.97	99.17
VEGDLKGPEADIK	13	1370.52	Neuroblast differentiation-associated protein AHNAK	−3.52	90
SMPGFKGEGPDGDVK	15	1520.68	Neuroblast differentiation-associated protein AHNAK	10.97	19.33
AGAISASGPELQGAGHSK	18	1637.77	Neuroblast differentiation-associated protein AHNAK	27.78	65.56
SPGAFTPLVKLER	13	1414.67	Decorin	27.75	90
QELRAHENEITKVR	14	1722.92	Decorin	38.43	83.57
LPKLDELR	8	983.18	Serum albumin	46.29	146.25
ARLSQRFPKAEF	12	1449.68	Serum albumin	41.27	49.17
TYSLGSALRPS	11	1151.28	Vimentin	61.62	80
VETRDGQVINETSQHHDDLE	20	2322.39	Vimentin	15.36	68
DEILPTTPISEQK	13	1470.64	40S ribosomal protein S3	83.31	90
GLTDTTVPR	9	950.07	40S ribosomal protein S6	5.21	75.56
GAKLTPEEEEILNKKR	16	1855.12	40S ribosomal protein S8	130	79.38
AQAAAPASVPAQAPK	15	1377.56	60S ribosomal protein L29	73.53	66
HQGVMVGMGQKDSY	14	1536.74	Actin, cytoplasmic 1	16.98	41.43
EGVVHGVATVAEK	13	1295.46	Alpha-synuclein	1.25	104.62
LGPLVEQGRVR	11	1223.44	Apolipoprotein E	26.6	123.64
ASGVAVSDGVIKV	13	1201.39	Cofilin-1	−3.83	134.62
GEGDFLAEGGGVR	13	1263.33	Fibrinogen alpha chain	16.62	60
KREEAPSLRPAPPPISGGG	19	1916.17	Fibrinogen beta chain	137.87	81.88
QGSHYEQLVDR	11	1331.41	Filaggrin	39.17	61.82
EHTYGQAGSQHEEPEFTVHER	21	2468.54	Filaggrin-2	40.44	18.57
VHNTHPRN	8	974.05	Follicle-stimulating hormone receptor	30.14	36.25
RVPTANVSVVDL	12	1269.46	Glyceraldehyde-3-phosphate dehydrogenase	12.69	137.5
DGLAHLDNLKGTFS	14	1487.63	Hemoglobin subunit delta	−6.16	90.71
KGEHPGLSIGDVAK	14	1407.59	High mobility group protein B1	−9.61	83.57
ALAAAGYDVEKNNS	14	1422.51	Histone H1.4	20.14	77.14
LAAGGYDVEK	10	1022.12	Histone H1.5	36.53	88
LYENRL	6	806.92	Leucine-rich repeat-containing protein 15	−4.23	130
AEGGGATTSTQVMVIKRPGR	20	2016.3	Methyl-CpG-binding protein 2	37.74	58.5
SEPQEVLHIGSAHNR	15	1673.81	PDZ and LIM domain protein 1	100.11	78
ALIDRPAPHFER	12	1421.62	Protein 4.1	42.39	81.67

(*continued on next page*)

Table 2 (*continued*)

Sequence	Length	Mass	Precursor protein	Instability index	Aliphatic index
FGQGGAGPVGGQGPR	15	1341.45	Splicing factor, proline- and glutamine-rich	22.28	26
YVVDSDTVQAHAAR	14	1531.65	Synaptopodin-2	−4.49	83.57
DGRPQVVPVEGPER	14	1534.69	Tenascin-X	71.34	62.14
VTEMRWPKQ	9	1174.38	Unmatched	102.43	32.33
PNIPLTEDSQYQNIMML	17	2007.3	Unmatched	98.6	91.76

Table 3
Selected endogenous peptides with high stability and fat solubility.

Peptides	Length (AA)	Molecular weight (Da)	Isoelectric point	Instability index	Aliphatic index	GRAVY	Precursor protein
ALTNAVAHVD	10	1010.11	5.08	−29.55	127	−0.67	Hemoglobin subunit alpha
ALTNAVAHVDD	11	1125.2	4.2	−25.95	115.45	0.291	Hemoglobin subunit alpha
ASGVAVSDGVIKV	13	1201.39	5.98	−3.83	134.62	1.162	Cofilin-1
LYENRL	6	806.92	6	−4.23	130	−0.867	Leucine-rich repeat-containing protein 15
PVNFKLLSH	9	1054.26	9.18	−12.54	118.89	0.178	Hemoglobin subunit alpha
VNFKLLSH	8	957.14	8.73	−39.44	133.75	0.4	Hemoglobin subunit alpha

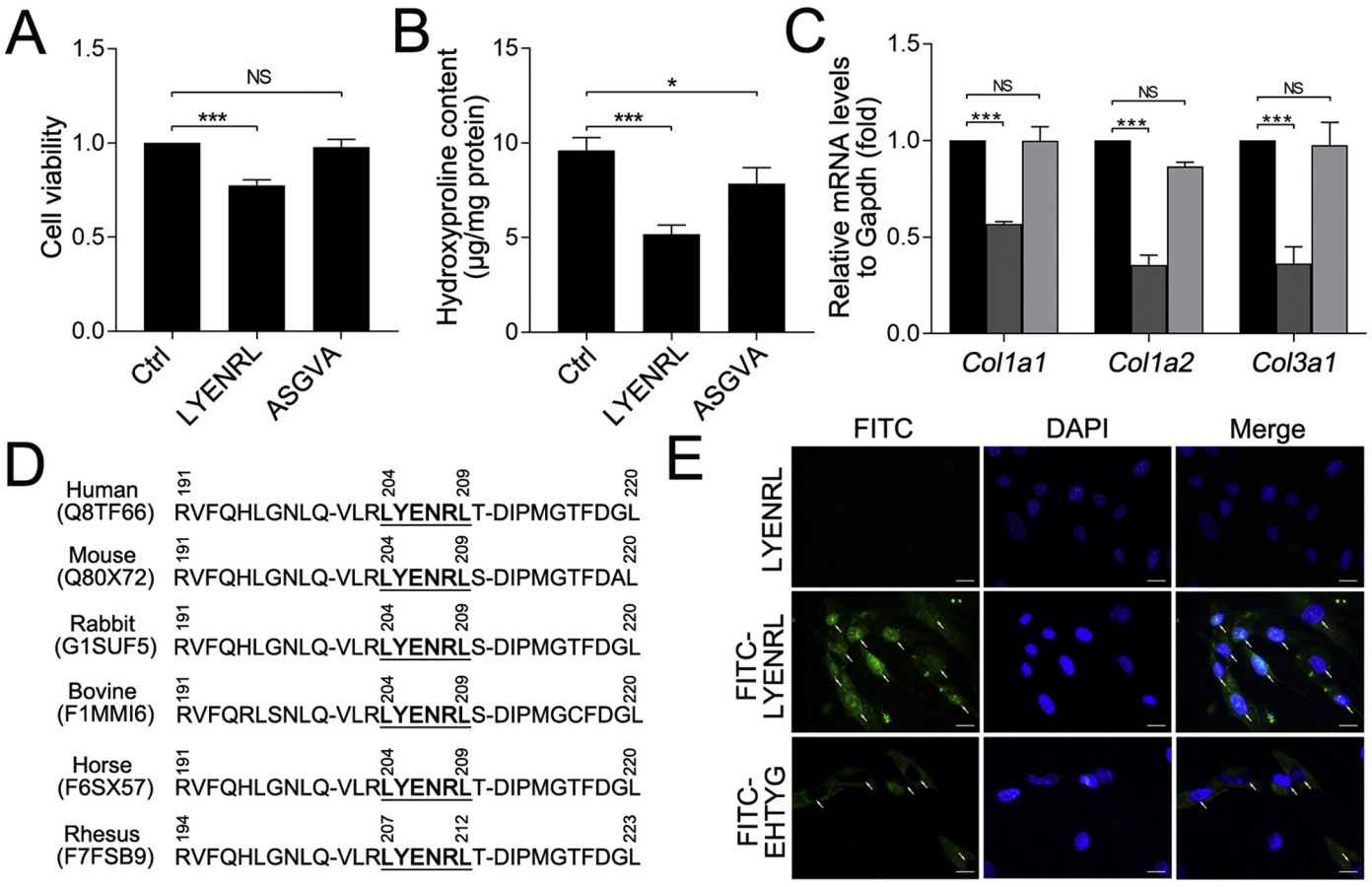

Fig. 2. LYENRL inhibits proliferation, hydroxyproline content and gene expression of collagens in human scar fibroblasts. (A–C) HSF cells were treated with solvent, LYENRL (50 μM) and ASGVA (50 μM) for 24 h. (A) Cell viability was measured by CCK-8 ($n = 3$). (B) Hydroxyproline content was measured ($n = 3$). (C) Representative RT-PCR for expression of *Col1a1*, *Col1a2* and *Col3a1* in HSF cells ($n = 3$). *Gapdh* served as the loading control. (D) Amino acid sequence alignment of LYENRL in human, mouse, rabbit, bovine, horse and rhesus. (E) Distributions of LYERNL and EHTYG in HSF cells after the cells treated with unlabeled LYENRL, FITC-labeled LYENRL or FITC-labeled EHTYG for 12 h. Scale bar, 20 μm. $^{*}P < 0.05$; $^{***}P < 0.001$; NS, not significant; by one-way ANOVA with LSD post hoc analysis for data meeting homogeneity of variance or with Dunnett's T3 analysis for data not assuming equal variances.

enhanced the activity of Smads. In contrast, LYENRL inhibited TGF-β1-induced Smad activity in a dose-dependent manner (Fig. 5F). Taken together, these results clarify the inhibitory effect of LYENRL on TGF-β1 signaling.

Since LYENRL exerts a direct inhibitory effect on TGF-β1/Smad signaling, we next investigated its effect on TGF-β1-induced scar hyperplasia. As shown in Fig. 6A and B, TGF-β1 stimulated the viability and proliferation of HSF cells, and LYENRL reversed these effects. Furthermore, LYENRL reduced expression of TGF-β1-induced collagen and fibrosis-related genes and the levels of hydroxyproline and the secreted form of type I collagen in cells, all in a dose-dependent manner (Fig. 6C–E). Finally, we assessed the effects of LYENRL on TGF-β1-

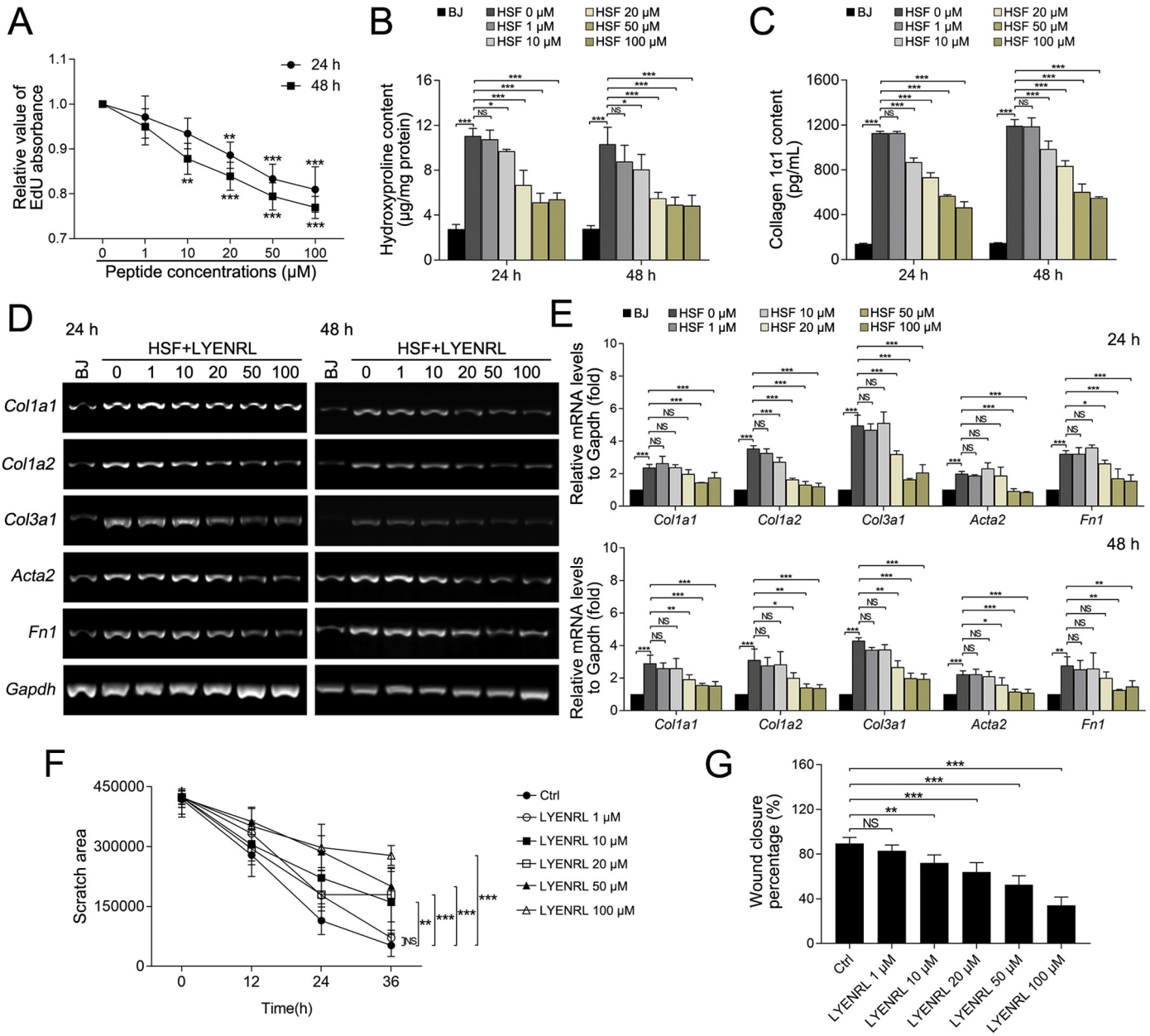

Fig. 3. LYENRL inhibits scar hyperplasia in vitro in a concentration dependent manner. (A) HSF cells were treated with solvent and different concentrations of LYENRL (1, 10, 20, 50 and 100 μM) for 24 h and 48 h, respectively. Cell proliferation was measured by EdU assay (n = 3). (B) Hydroxyproline content in HSF cells treated with different concentrations of LYENRL (1, 10, 20, 50 and 100 μM) and BJ cells for 24 h and 48 h. (C) Secretion of collagen 1α1 was measured by ELISA in HSF cells treated with different concentrations of LYENRL (1, 10, 20, 50 and 100 μM) and BJ cells for 24 h and 48 h (n = 3). (D) Gene expression of *Col1a1*, *Col1a2*, *Col3a1*, *Acta2* and *Fn1* in HSF cells treated with different concentrations of LYENRL (1, 10, 20, 50 and 100 μM) and BJ cells for 24 h and 48 h was measured by RT-PCR. (E) Relative gray values of the bands showed in D. *Gapdh* served as the loading control (n = 3). (F, G) HSF cells were treated with different concentrations of LYENRL after scratching, and the degree of wound closure was recorded after 12 h, 24 h and 36 h, subsequently the scratched areas were measured and the wound closure percentage were calculated (five scratch pictures for each group at each time point were selected for data analysis, and three independent experiments were performed). $^{*}P < 0.05$; $^{**}P < 0.01$; $^{***}P < 0.001$, compared with the cells treated with solvent (A); $^{*}P < 0.05$; $^{**}P < 0.01$; $^{***}P < 0.001$; NS, not significant (B–G); by one-way ANOVA with LSD post hoc analysis for data meeting homogeneity of variance or with Dunnett's T3 analysis for data not assuming equal variances.

induced HSF cell migration and invasion. TGF-β1 treatment slightly improved the migration ability of HSF cells (Fig. 6F, G and Fig. S2A). Different from the ability of LYENRL to promote cell migration, LYENRL promoted the invasion of HSF cells, as shown in the transwell experiment (Fig. 6H). However, LYENRL antagonized the scratch healing rate of HSF cells induced by TGF-β1 (Fig. 6F and G) and almost completely reversed TGF-β1-induced invasion of HSF cells (Fig. 6H). Based on the results above, we conclude that the endogenous peptide LYENRL can inhibit the proliferation, collagen synthesis and secretion, migration and invasion of fibroblasts originating from human hypertrophic scar tissues by inhibiting the activation of the TGF-β1/Smad signaling pathway. Thereby, LYENRL is most likely a candidate compound for scar hyperplasia treatment.

3.5. LYENRL inhibits *Tgfb1* gene transcription by preventing AP-1 binding to the promoter

LYENRL inhibited gene expression of *Tgfb1* and decreased secretion of TGF-β1 in the culture medium. To investigate the mechanism of how LYENRL downregulated *Tgfb1* gene expression, ActD gene inhibition

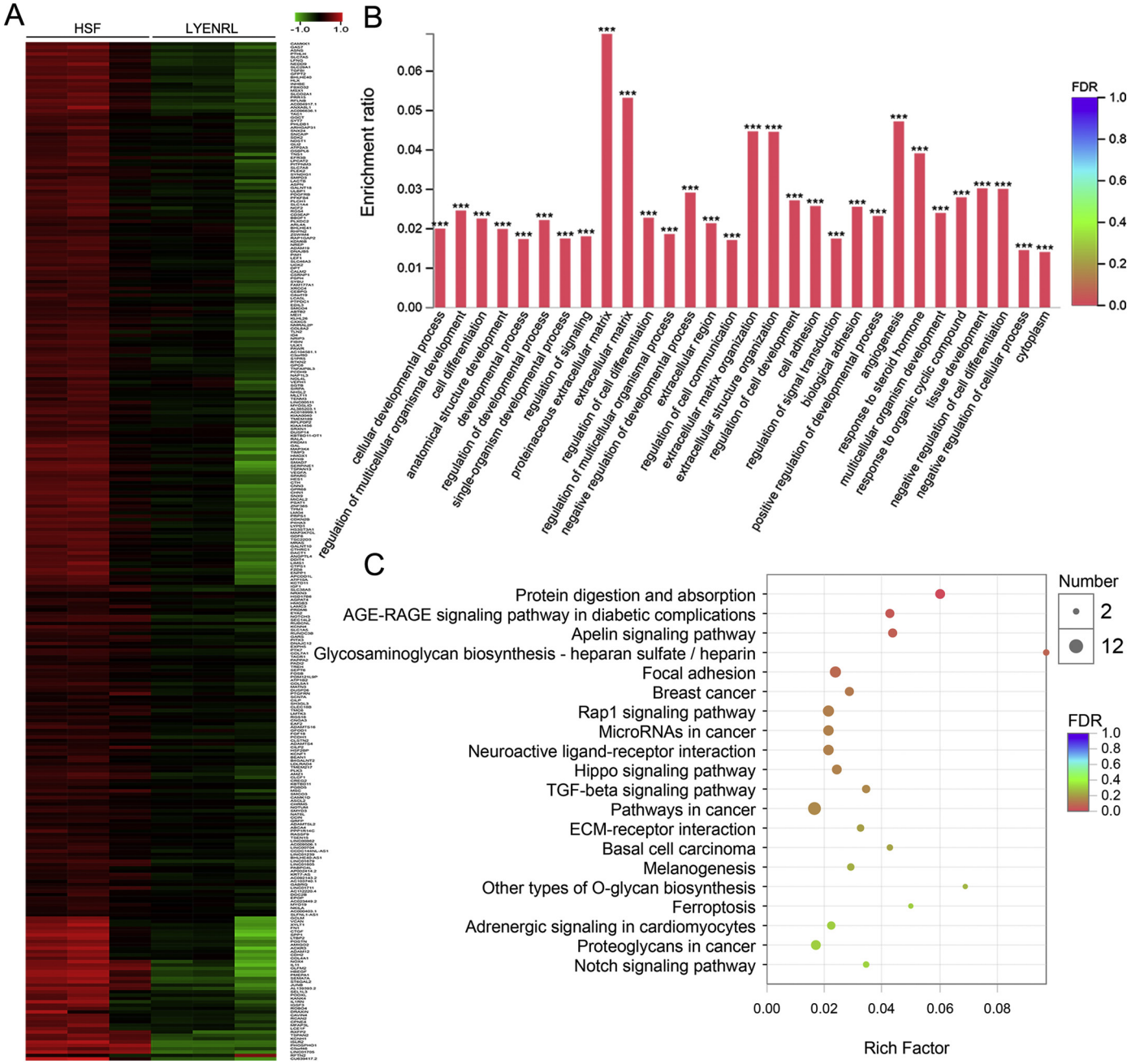

Fig. 4. Transcriptome sequencing analysis of LYENRL on HSF cells. HSF cells were treated with LYENRL (50 μM) or solvent for 24 h, total RNA was isolated from the cells and transcriptome sequencing analysis was performed. Samples from three independent experiments were performed in each group. HSF cells treated with solvent were served as the control. (A) Clustering of gene set downregulated by LYENRL in HSF cells. (B) GO functional analysis of the LYENRL downregulated gene set (showing the top 30 biological processes with the highest enrichment ratio). (C) KEGG analysis of the LYENRL downregulated gene set (showing the top 20 pathways with the highest rich factor and related gene numbers).

experiments were performed. When global gene transcription in HSF cells was prevented by ActD, LYENRL was unable to inhibit mRNA levels of *Tgfb1*, whose expression was inhibited in the absence of ActD (Fig. 7A). On the other hand, the degradation of *Tgfb1* mRNA was not affected by LYENRL treatment after gene transcription suspension by ActD (Fig. 7B). These results indicated that LYENRL downregulated gene expression of *Tgfb1* at the transcriptional level. To further confirm the inhibitory effect of LYENRL on the transcriptional levels of *Tgfb1*, we constructed a luciferase reporter vector containing the *Tgfb1* promoter and found that LYENRL was capable of reducing the promoter activity of *Tgfb1* in a concentration-dependent manner (Fig. 7C). To identify the region where LYENRL acts on the *Tgfb1* promoter, *Tgfb1* reporter vector variants of different lengths were constructed (Fig. 7D, left). The results revealed that the region between −618 and –386 was crucial to the inhibitory effects of LYENRL on the transcriptional activity of *Tgfb1* (Fig. 7D, right). Through bioinformatics analysis (PROMO and JASPAR databases), we found that early growth response 1 (Egr1) and AP-1 are specific transcription factor binding sites in pTgfb1-618 (Fig. S2B). The inhibitory effects of LYENRL on the *Tgfb1* promoter transactivation were largely reversed when the AP-1 binding site, but not the Egr1 binding site was mutated (Fig. 7E), suggesting the necessary effect of AP-1. Considering the fact that AP-1 is classically a heterodimer between c-Jun and c-Fos, we also measured the gene expression of *Egr1*, *Jun* and *Fos*. However, LYENRL did not exert an

Table 4
Effects of LYENRL on expression of genes related to TGF-β signaling pathway.

Gene name	HSF_1	HSF_2	HSF_3	LYENRL_1	LYENRL_2	LYENRL_3
Tgfb1	272.47	240.75	481.81	73.27	68.18	158.91
Tgif1	149.7	150.04	35.86	92.32	94.24	9.97
Tgif2	5	6.6	2.94	6.02	3.09	1.85
Smad1	6.54	12.51	0.3	11.82	13.68	0.11
Smad2	43.25	57.95	8.68	50.87	48.74	6.04
Smad3	20.59	29.3	5.6	66.7	72.38	15.94
Smad4	32.79	48.62	1.83	33.34	33.25	0.72
Smad5	11.64	25.29	2.08	14.29	18.09	0.69
Smad7	83.12	80.36	27.7	24.54	20.87	1.31
Cdkn2b	39.38	42.3	6.53	13.65	8.25	0.67
Gdf1	3.07	2.86	2.26	0.09	1.33	4.3
Gdf6	38.11	45.87	18.36	5.91	7.31	1.39
Inhbe	15.51	20.14	6.14	3.28	1.58	0.54
Lefty2	3.18	2.51	2.95	0	0	0.02
Rhoa	566.62	557.23	204.88	418.83	430.21	111.98

obvious effect on gene expression of *Egr1*, *Jun or Fos* (Figs. 7F and S2C), indicating that LYENRL may not regulate *Tgfb1* transcription activity through directly affecting gene expression of transcription factors. Considering that transcription factors regulate gene transcription through binding with the promoter, the binding activities of these three transcription factors were examined by chromatin immunoprecipitation (ChIP), and the results revealed that LYENRL inhibited the binding activity of both c-Jun and c-Fos to the *Tgfb1* promoter but had no effect on the binding activity of Egr1 (Fig. 7G). Taken together, LYENRL inhibits the transcriptional activity of *Tgfb1* by reducing the binding of AP-1 to the *Tgfb1* promoter.

4. Discussion

Many stimuli, such as physical trauma, surgical incision and burn injuries can cause skin damage and lead to the development of hypertrophic scars or keloids. In developed countries, approximately 100 million people suffer from scar related problems each year [19]. Scars cause changes in appearance, restriction of movement and pain, significantly affecting patient quality of life, physical state and mental health [21]. At present, intralesional steroid injection, surgical resection, cryotherapy, radiation and laser therapies are the primary strategies for hypertrophic scar treatment. However, a series of adverse reactions, such as skin atrophy, high recurrence rate or damage to other tissues, can occur after these treatments ([22–26]. Therefore, understanding the mechanism of hypertrophic scar establishment and identifying new targets for hypertrophic scar treatment is becoming a hot topic in the field of scar treatment.

Hypertrophic scar formation is a fibroproliferative disorder caused by abnormal healing of the wound, whose pathology contains three classic stages, the inflammatory phase, the proliferative phase and the remodeling phase [27]. The inflammatory phase is the first period of wound healing, which occurs immediately after tissue injury and lasts for a short time [28]. During the proliferative phase, mainly characterized by proliferation and migration of active cells, a portion of fibroblasts are able to transform into myofibroblasts, thus producing ECM (mainly in the form of collagens) and leading to the formation of scar [29]. Once the wound is closed, the remodeling phase begins, manifesting as degeneration of excess tissue and transformation of immature wound healing products into mature forms [30]. Among these three phases, fibroblast proliferation and excessive ECM production are pathological processes of hypertrophic scar formation [31].

Peptides play crucial roles in a variety of biological processes [4]. Moreover, the roles of these peptides in hypertrophic scar formation have been frequently studied. TGF-β peptide antagonist and human recombinant peptide IL-10-RGD have been confirmed to have therapeutic effects on hypertrophic scars [32,33]. Recent studies demonstrated that endogenous peptides, small peptides with 3 to 50 amino acids originating from endocrine glands, organs, cells or body fluids, are involved in various physiological and pathological processes, including immune regulation, tissue remodeling, and nervous system and renal diseases ([34–37]. In addition, peptide drugs are expected to become a novel choice for disease treatment because of their unique advantages, such as low toxicity, high specificity, small molecular weight and easy entry into cells [38]. However, the roles of endogenous peptides in hypertrophic scars remain poorly understood.

In our previous study, we identified 1679 endogenous peptides in scar tissues and the surrounding normal tissues. However, the biological functions of these differentially expressed peptides have not been studied [15]. In this study, peptidomics results from our previous study were used as an entry point to identify potential endogenous peptides that inhibit hypertrophic scars. Of the 1679 endogenous peptides, we focused on 78 peptides that were minimally expressed in scar tissues. LYENRL, a small and short peptide, inhibited the activation of scar fibroblasts, which is an important process in the pathogenesis of hypertrophic scars, characterized as the prevention of cell proliferation, hydroxyproline production and type I/III collagen gene expression. Coincidentally, this endogenous peptide is conserved in many species, establishing a good foundation for subsequent animal experiments. In addition, consistent with bioinformatics analysis, this peptide can easily penetrate into the cytoplasm and enter into the nucleus of fibroblasts, providing conveniences for its biological function. Further experiments

Table 5
Effects of LYENRL on expression of genes related to collagen and fibrosis.

Gene name	HSF_1	HSF_2	HSF_3	LYENRL_1	LYENRL_2	LYENRL_3
Col1a1	10,102.66	13,811.63	12,466.07	2261.1	2951.54	5443.56
Col1a2	4246.53	4731.97	1839.96	2575.78	2774.87	918.1
Col2a1	0.05	0.62	0.1	0.14	0.16	0
Col3a1	458.39	563.99	155.75	180.09	141.95	82.05
Col4a1	225.36	343.43	69.45	56.73	65.72	7.22
Col4a2	325.41	368.94	306.77	136.33	133.84	86.74
Col5a1	985.94	1210.43	864.45	255.95	297.07	215.78
Col5a2	228.58	314.78	47.86	155.35	187.07	25.14
Col6a1	1657.37	1728.96	582.92	1929.03	1913.26	577.61
Col6a2	1603.19	1617.84	1282.54	1777.43	1731.24	1964.64
Col6a3	1745.15	2554.97	253.23	513.22	608.91	34.64
Col7a1	294.64	284.95	198.89	86.67	85.92	79.23
Col8a1	163.36	249.83	23.21	104.21	115.57	3.65
Col8a2	11.48	13.44	6.5	2.29	2.39	1
Acta2	229.45	234.19	182.81	153.58	153.23	86.26
Ctgf	1242.81	1361.83	251.49	120.78	138.67	14.14
Fn1	7547.92	8101.4	1792.22	1105.45	1105.33	148.05
Vegf	116.49	136.03	40.27	39.23	40.23	6.55

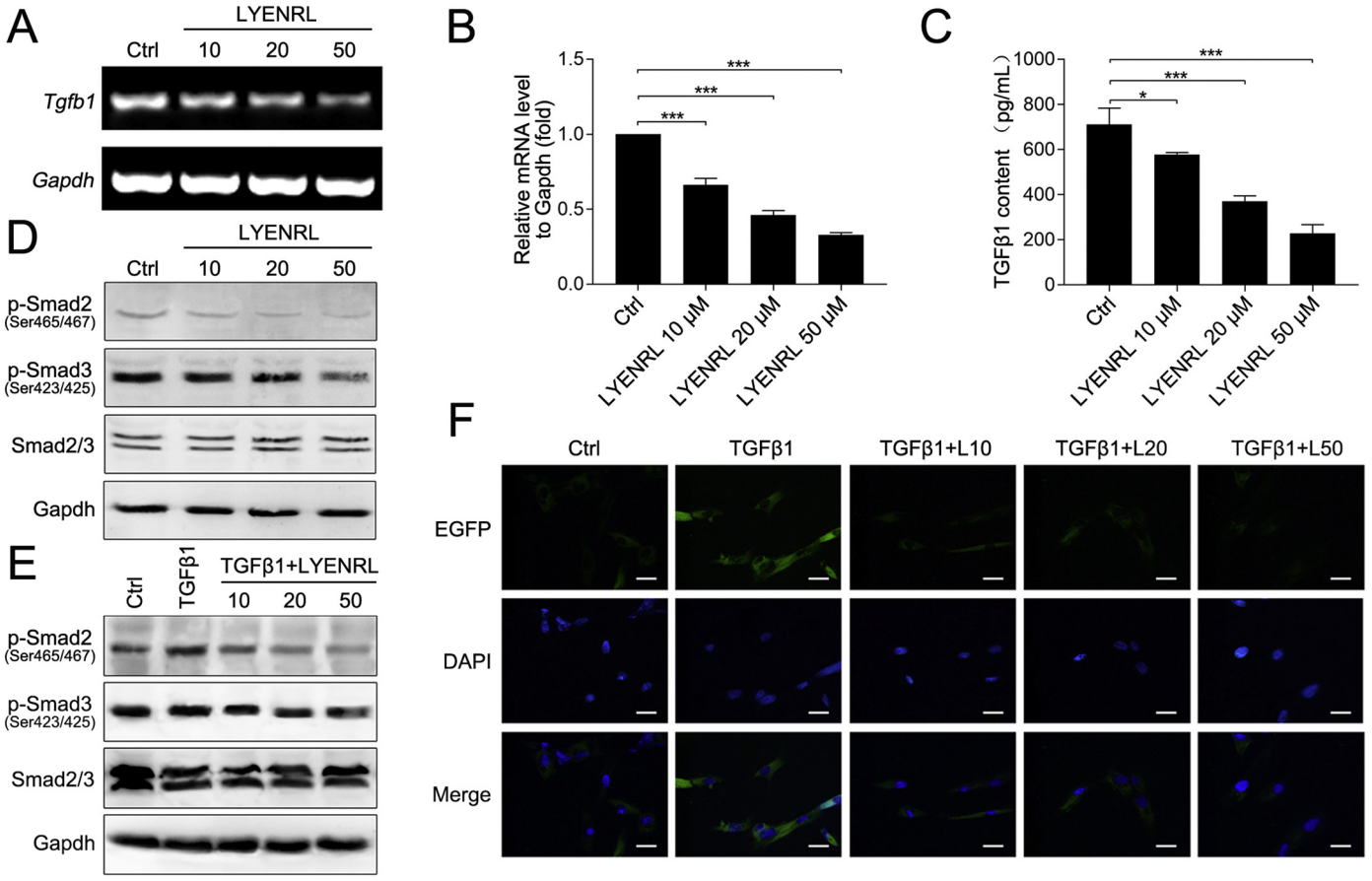

Fig. 5. Inhibitory effects of LYENRL on TGF-β1 signaling pathway. (A-D) HSF cells were treated with solvent and different concentrations of LYENRL (10, 20 and 50 μM) for 24 h. (A and B) Gene expression of *Tgfb1* in HSF cells was measured by RT-PCR. *Gapdh* served as the loading control ($n = 3$). (C) TGF-β1 content in the cell culture medium was detected using ELISA ($n = 3$). (D) Phosphorylation levels of Smad2 and Smad3 were examined by western blotting, and Gapdh served as the loading control. (E) HSF cells were treated with solvent, TGF-β1 (5 ng/mL) and different concentrations of LYENRL (10, 20 and 50 μM) combined with TGF-β1 for 24 h. Phosphorylation levels of Smad2 and Smad3 were measured by western blotting, and Gapdh served as the loading control. (F) HSF cells were previously transfected with EGFP-Smad reporter plasmids for 24 h, then the cells were treated with solvent, TGF-β1 (5 ng/mL) and different concentrations of LYENRL (10, 20 and 50 μM) combined with TGF-β1 for 24 h. Fluorescence microscopy was used to detect EGFP and nuclei. Scale bar, 20 μm. $^{*}P < 0.05$; $^{***}P < 0.001$; by one-way ANOVA with LSD post hoc analysis for data meeting homogeneity of variance or with Dunnett's T3 analysis for data not assuming equal variances.

demonstrated that LYENRL acts to substantially inhibit the proliferation, migration, collagen and fibrosis-related gene expression, and type I collagen secretion at 10 μM, which is a low concentration for peptide treatment. However, little difference was seen between treatment for 24 h and 48 h, which may be related to the stability of the peptide. It is predicted that the half-life of LYENRL is 5.5 h and prolonged action may lead to degradation. Subsequently, to maximize the efficiency, the identification of suitable chemical modification methods to increase the stability of the peptide may be worth pursuing. Owing to characteristics of this peptide, such as small molecular size and easy access to cells, it may have a nonspecific effect on other cell types, although we did not observe the effects of this peptide on BJ cells in this study. However, if the peptide's druggability is assessed in the future, it will formulate as a topical drug for administration on hypertrophic scars to minimize the nonspecific effect of the peptide on other cell types in the skin.

To investigate the molecular mechanisms by which LYENRL works, we performed transcriptome sequencing analysis of LYENRL treated scar fibroblasts. GO analysis of LYENRL downregulated genes revealed that these genes are mainly associated with ECM and angiogenesis. As mentioned above, ECM is the main substance produced by fibroblasts during wound healing and is one of the principal factors leading to hypertrophic scar formation. ECM is mainly present in the form of collagens, as well as elastin, hyaluronic acid and proteoglycans [29]. Table 5 lists the gene expression of major extracellular matrix factors from transcriptome sequencing, LYENRL inhibits gene expression of type I, type III, type IV and type V collagens. In addition, gene expression of fibrosis-related genes *Acta2*, *Ctgf* and *Fn1* is also suppressed, which was further verified by PCR. Moreover, angiogenesis is associated with scar hyperplasia. Studies have shown that vascular epidermal growth factor (VEGF) overexpression can lead to excessive capillary formation, thus promoting the formation of type I collagen and increasing scar volume [39]. In this study, transcriptome sequencing results revealed that LYENRL reduces the expression of *Vegf* in HSF cells (Table 5).

The TGF-β signaling pathway is most closely related to scar hyperplasia among the main enrichment pathways of LYENRL downregulated genes. After binding of TGF-β1 to the TGF-β receptor, Smad2/3 was phosphorylated, followed by binding with Smad4 to form a heterotrimer that transfers to the nucleus. The Smad2/3/4 heterotrimer binds to Smad binding elements (SBE) on the promoters of target genes, regulating target gene transcription and promoting dermal fibroblast proliferation and ECM production ([40,41]. Key target genes of the TGF-β signaling pathway listed in Table 4 showed that LYENRL reduced gene expression of *Tgfb1* but only weakly affected gene expression of TGF-β1 inducing factor (*Tgif*) and *Smads*. Interestingly, the expression of the TGF-β signaling pathway target genes *Cdkn2b*, *Gdf1*, *Gdf6*, *Inhbe*, *Lefty 2* and *Rhaa* was also notably inhibited. These results indicated that LYENRL may inhibit *Tgfb1* gene expression at the source, thereby inhibiting the activation of the TGF-β signaling pathway. In vitro experiments demonstrated that *Tgfb1* gene expression and TGF-β1

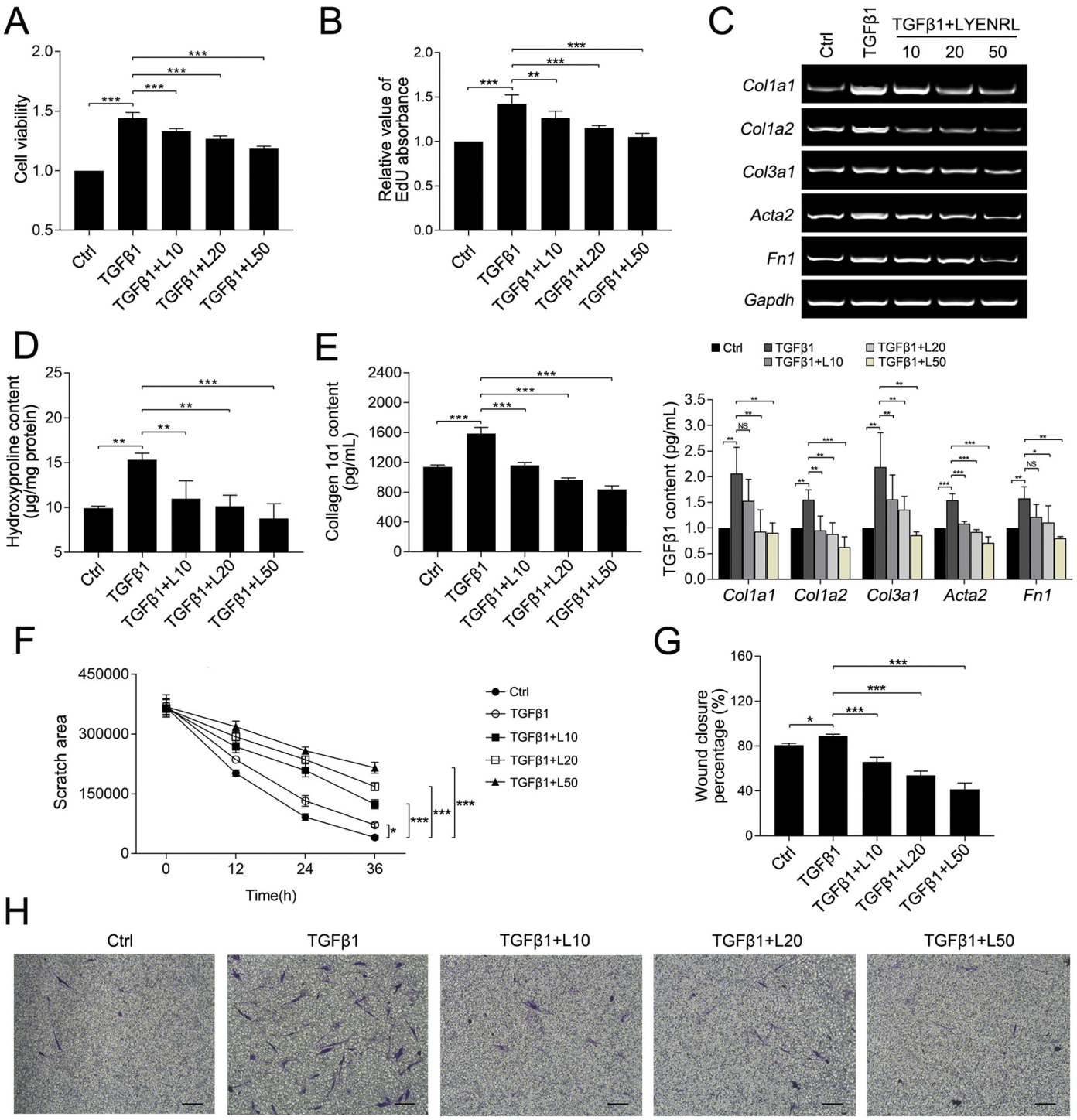

Fig. 6. LYENRL inhibits TGF-β1-induced scar fibroblasts activation. HSF cells were treated with solvent, TGF-β1 (5 ng/mL) and different concentrations of LYENRL (10, 20 and 50 μM) combined with TGF-β1 for 24 h. (A) Cell viability was measured by CCK-8 ($n = 3$). (B) Cell proliferation was measured by EdU assay ($n = 3$). (C) Gene expression of *Col1a1*, *Col1a2*, *Col3a1*, *Acta2* and *Fn1* in HSF cells was measured by RT-PCR. *Gapdh* served as the loading control ($n = 3$). (D) Hydroxyproline content in HSF cells was measured by a commercial kit ($n = 3$). (E) Collagen 1α1 secretion of HSF cells was measured by ELISA ($n = 3$). (F, G) HSF cells were treated with solvent, TGF-β1 (5 ng/mL) and different concentrations of LYENRL (10, 20 and 50 μM) combined with TGF-β1 after scratching, and the degree of wound closure was recorded after 12 h, 24 h and 36 h, subsequently the scratched areas were measured and the wound closure percentage were calculated (five scratch pictures for each group at each time point were selected for data analysis). (H) HSF cells were inoculated into the transwell chamber before treated with TGF-β1 and different concentrations of LYENRL stated above for 24 h, subsequently, cells were stained according to the protocol and were photographed under an inverted microscope. Scale bar, 50 μm. $^{*}P < 0.05$; $^{**}P < 0.01$; $^{***}P < 0.001$; NS, not significant; by one-way ANOVA with LSD post hoc analysis for data meeting homogeneity of variance or with Dunnett's T3 analysis for data not assuming equal variances.

secretion were also decreased in response to LYENRL treatment. Although it had no effect on gene expression of Smads, LYENRL reduced Smad2/3 phosphorylation and inhibited binding of the Smad2/3/4 complex to SBE. In addition, LYENRL reversed TGF-β1-induced scar fibroblast proliferation, collagen synthesis and secretion, invasion and migration, suggesting that LYENRL may reduce TGF-β1 protein

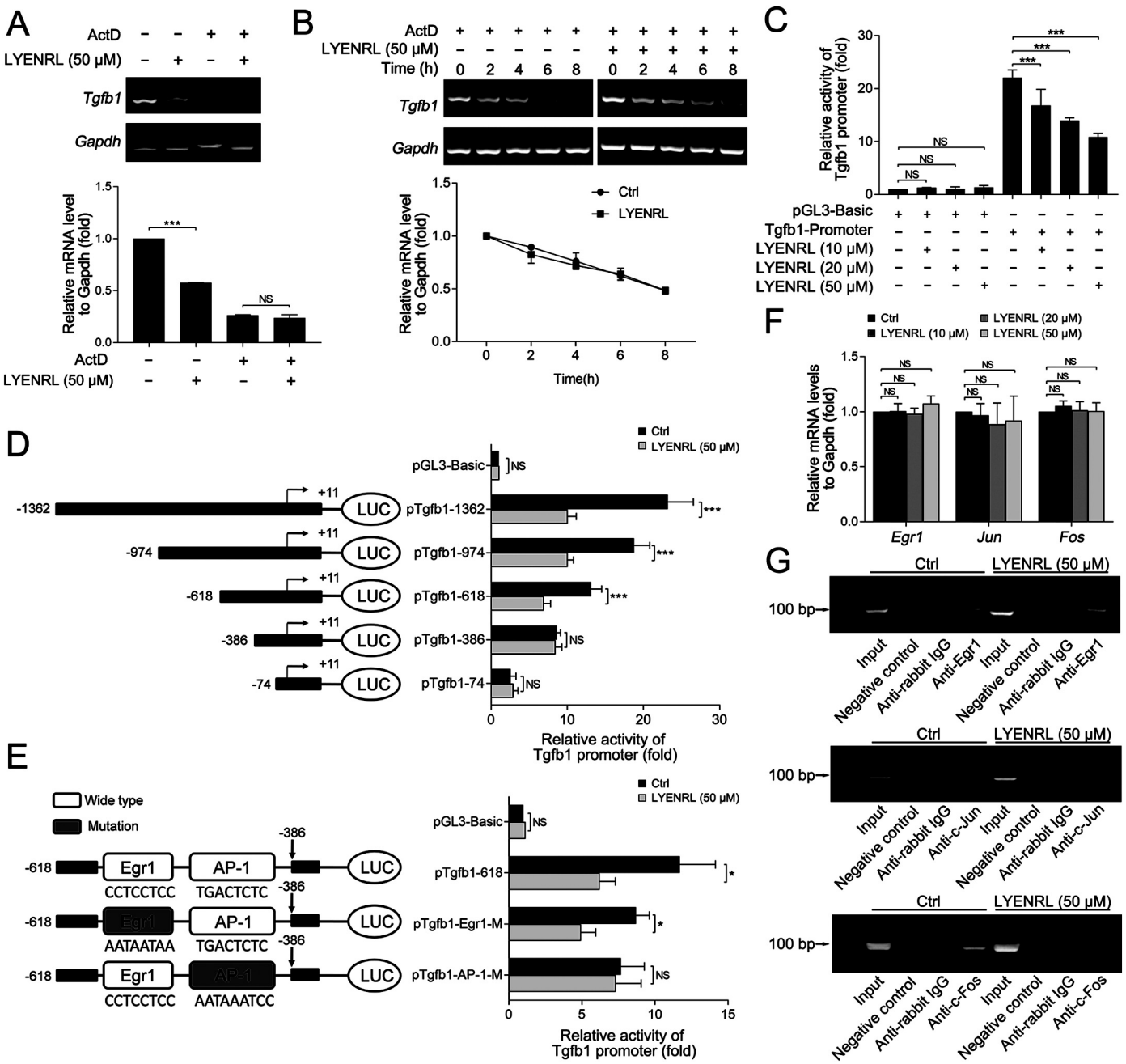

Fig. 7. LYENRL inhibits *Tgfb1* gene transcription by preventing AP-1 binding with the promoter. (A) HSF cells were treated with ActD (5 μg/mL) for 6 h, then the cells were treated with LYENRL (50 μM) for another 24 h. Gene expression of *Tgfb1* was measured by RT-PCR ($n = 3$). *Gapdh* served as the loading control. (B) HSF cells were treated with solvent or LYENRL (50 μM) for 24 h, then the cells were treated with ActD (5 μg/mL) for 2 h, 4 h, 6 h and 8 h, respectively. Gene expression of *Tgfb1* was measured by RT-PCR ($n = 3$). *Gapdh* served as the loading control. (C) HSF cells were transiently transfected with pGL3-Basic (0.8 μg) or pTgfb1 (0.8 μg) and pRL plasmid (0.08 μg) for 24 h, then the cells were treated with solvent or different concentrations of LYENRL (10, 20 and 50 μM) for another 24 h. The luciferase activity was measured according to the protocols ($n = 3$). (D) Construction of *Tgfb1* promoter reporter plasmid and its deletion mutants (Left). HSF cells were transiently transfected with indicated plasmids (0.8 μg) and pRL plasmid (0.08 μg) for 24 h, then the cells were treated with solvent or LYENRL (50 μM) for another 24 h. The luciferase activity was measured according to the protocols ($n = 3$) (right). (E) Construction of variants of pTgfb1-618 with point mutations in indicated sites (Left). HSF cells were transiently transfected with indicated plasmids (0.8 μg) and pRL plasmid (0.08 μg) for 24 h, then the cells were treated with solvent or LYENRL (50 μM) for another 24 h. The luciferase activity was measured according to the protocols ($n = 3$) (right). (F) HSF cells were treated with solvent or different concentrations of LYENRL (10, 20 and 50 μM) for 24 h. Gene expression of *Egr1*, *Jun* and *Fos* was measured by RT-PCR ($n = 3$). *Gapdh* served as the loading control. (G) HSF cells were treated with solvent or LYENRL (50 μM) for 24 h. Binding of Egr1, c-Jun and c-Fos with *Tgfb1* promoter was assessed in a ChIP assay according to the protocol. IgG was used as a non-specific control. $^{*}P < 0.05$; $^{***}P < 0.001$; NS, not significant; by one-way ANOVA with LSD post hoc analysis for data meeting homogeneity of variance or with Dunnett's T3 analysis for data not assuming equal variances (A, C, F); two-tailed Student's *t*-test (D, E).

expression and release by inhibiting *Tgfb1* gene expression, thereby inhibiting activation of the TGF-β1 signaling pathway from the source.

Through ActD experiments, we determined that LYENRL regulates *Tgfb1* gene expression at the transcriptional level. Furthermore, we confirmed the region regulated by LYENRL to be in the −618 to −386 bp region of the *Tgfb1* promoter by analyzing luciferase activity of its deletion mutation. The heterodimer AP-1 plays a crucial role in the downregulation of *Tgfb1* transcriptional activity by LYENRL as the

mutation of the AP-1 binding site reversed the inhibitory effects of LYENRL on the transcriptional activity of *Tgfb1*. In addition, treatment with LYENRL reduced the combination of c-Jun and c-Fos (two components of AP-1) with the *Tgfb1* promoter. Studies have shown that AP-1 plays a key role in the transcription of the *Tgfb1* gene. For example, *C. butyricum* activates Toll-like receptor 2 (TLR2), thereby activating the *Tgfb1* promoter activity via ERK-AP-1 signaling [42]. In addition, polyamides designed across the AP-1 binding site have also been shown to inhibit the promoter activity of *Tgfb1* in rat scar skin, ultimately preventing effective scar formation [43].

In summary, this study identified an endogenous peptide, LYENRL, by means of peptidomics. This peptide inhibited the proliferation of fibroblasts and reduced the production of ECM by fibroblasts, which are the most critical nodes of pathology in hypertrophic scars. In addition, this peptide works by hindering the binding of AP-1 heterodimer to the *Tgfb1* promoter, inhibiting *Tgfb1* transcription, and reducing TGF-β1 protein expression and secretion, thereby inhibiting the activation of TGF-β1/Smad signaling at the source. We believe that appropriate chemical modification of LYENRL to increase its stability and specificity for the *Tgfb1* promoter will help it become a promising peptide for hypertrophic scar treatment.

Supplementary data to this article can be found online at https://doi.org/10.1016/j.lfs.2019.116674.

Author contributions

X.J.J. designed and performed experiments, analyzed data and wrote the manuscript; Z.T. examined the endogenous peptides using LC/MS; W.W.S. and L.C. constructed the plasmids used in cell experiments and was responsible for cell culture; Z.R.Z. helped in the data analysis and revised the manuscript. J.Y.L. and L.C. guided the experimental design and helped in the data analysis; J.C. provide financial support and participated in the experimental design; W.Y. supervised the study, designed the experiments and wrote the manuscript.

Acknowledgements

This project was sponsored by the National Natural Science Fund of China (81703100, 81673462, 81473293, 81403347, 81573604, and 91540119), the Fundamental Research Funds for the Central Universities. Six Talent Peaks Project in Jiangsu Province to Y.W. (YY-012). Key Research and Development Project of Jiangsu Province (BE2017712). The Science and Technology Development Foundation of Nanjing Medical University (2017NJMUZD065).

Declaration of Competing Interest

The authors declared that there are no competing interests associated with the manuscript.

References

[1] C.C. Finnerty, M.G. Jeschke, L.K. Branski, J.P. Barret, P. Dziewulski, D.N. Herndon, Hypertrophic scarring: the greatest unmet challenge after burn injury, Lancet (London, England) 388 (2016) 1427–1436.
[2] C. Profyris, C. Tziotzios, I. Do Vale, Cutaneous scarring: pathophysiology, molecular mechanisms, and scar reduction therapeutics part I. the molecular basis of scar formation, J. Am. Acad. Dermatol. 66 (2012) 1–10.
[3] D. Wolfram, A. Tzankov, P. Pulzl, H. Piza-Katzer, Hypertrophic scars and keloids–a review of their pathophysiology, risk factors, and therapeutic management, Dermatologic Surgery: Official Publication for American Society for Dermatologic Surgery [et Al] 35 (2009) 171–181.
[4] D.C. Dallas, A. Guerrero, E.A. Parker, R.C. Robinson, J. Gan, J.B. German, et al., Current peptidomics: applications, purification, identification, quantification, and functional analysis, Proteomics 15 (2015) 1026–1038.
[5] M. Riemenschneider, N. Lautenschlager, S. Wagenpfeil, J. Diehl, A. Drzezga, A. Kurz, Cerebrospinal fluid tau and beta-amyloid 42 proteins identify Alzheimer disease in subjects with mild cognitive impairment, Arch. Neurol. 59 (2002) 1729–1734.
[6] D.M. Good, P. Zurbig, A. Argiles, H.W. Bauer, G. Behrens, J.J. Coon, et al., Naturally occurring human urinary peptides for use in diagnosis of chronic kidney disease, Molecular & Cellular Proteomics: MCP 9 (2010) 2424–2437.
[7] J. Metzger, T. Kirsch, E. Schiffer, P. Ulger, E. Mentes, K. Brand, et al., Urinary excretion of twenty peptides forms an early and accurate diagnostic pattern of acute kidney injury, Kidney Int. 78 (2010) 1252–1262.
[8] K. Rossing, H. Mischak, H.H. Parving, P.K. Christensen, M. Walden, M. Hillmann, et al., Impact of diabetic nephropathy and angiotensin II receptor blockade on urinary polypeptide patterns, Kidney Int. 68 (2005) 193–205.
[9] D. Theodorescu, E. Schiffer, H.W. Bauer, F. Douwes, F. Eichhorn, R. Polley, et al., Discovery and validation of urinary biomarkers for prostate cancer, Proteomics Clin. Appl. 2 (2008) 556–570.
[10] L.U. Zimmerli, E. Schiffer, P. Zurbig, D.M. Good, M. Kellmann, L. Mouls, et al., Urinary proteomic biomarkers in coronary artery disease, Molecular & Cellular Proteomics: MCP 7 (2008) 290–298.
[11] G. Baggerman, K. Boonen, P. Verleyen, A. De Loof, L. Schoofs, Peptidomic analysis of the larval Drosophila melanogaster central nervous system by two-dimensional capillary liquid chromatography quadrupole time-of-flight mass spectrometry, Journal of Mass Spectrometry: JMS 40 (2005) 250–260.
[12] X.B. Ji, J. Luo, X.L. Feng, Q.L. Xu, T. Man, D. Zhao, et al., The immunomodulatory peptide bursopentin (BP5) enhances proliferation and induces sIgM expression in DT40 cells, Afr. Health Sci. 18 (2018) 1292–1302.
[13] I.D. Vats, S. Chaudhary, J. Karar, M. Nath, Q. Pasha, S. Pasha, Endogenous peptide: met-enkephalin-Arg-Phe, differently regulate expression of opioid receptors on chronic treatment, Neuropeptides 43 (2009) 355–362.
[14] X.J. Zeng, S.P. Yu, L. Zhang, L. Wei, Neuroprotective effect of the endogenous neural peptide apelin in cultured mouse cortical neurons, Exp. Cell Res. 316 (2010) 1773–1783.
[15] J. Li, L. Chen, Q. Li, J. Cao, Y. Gao, J. Li, Comparative peptidomic profile between human hypertrophic scar tissue and matched normal skin for identification of endogenous peptides involved in scar pathology, J. Cell. Physiol. 233 (2018) 5962–5971.
[16] R.E. Neuman, M.A. Logan, The determination of hydroxyproline, J. Biol. Chem. 184 (1950) 299–306.
[17] Q. Lu, X.J. Ji, Y.X. Zhou, X.Q. Yao, Y.Q. Liu, F. Zhang, et al., Quercetin inhibits the mTORC1/p70S6K signaling-mediated renal tubular epithelial-mesenchymal transition and renal fibrosis in diabetic nephropathy, Pharmacol. Res. 99 (2015) 237–247.
[18] C. Dan, B. Jinjun, H. Zi-Chun, M. Lin, C. Wei, Z. Xu, et al., Modulation of TNF-alpha mRNA stability by human antigen R and miR181s in sepsis-induced immunoparalysis, EMBO Molecular Medicine 7 (2015) 140–157.
[19] H.J. Lee, Y.J. Jang, Recent understandings of biology, prophylaxis and treatment strategies for hypertrophic scars and keloids, Int. J. Mol. Sci. 19 (2018).
[20] R.E. Neuman, M.A. Logan, The determination of collagen and elastin in tissues, J. Biol. Chem. 186 (1950) 549–556.
[21] R.S. Chiang, A.A. Borovikova, K. King, D.A. Banyard, S. Lalezari, J.D. Toranto, et al., Current concepts related to hypertrophic scarring in burn injuries, Wound Repair and Regeneration: Official Publication of the Wound Healing Society [and] the European Tissue Repair Society 24 (2016) 466–477.
[22] C. Boyadjiev, E. Popchristova, J. Mazgalova, Histomorphologic changes in keloids treated with Kenacort, J. Trauma 38 (1995) 299–302.
[23] M.L. Elsaie, S. Choudhary, Lasers for scars: a review and evidence-based appraisal, Journal of Drugs in Dermatology: JDD 9 (2010) 1355–1362.
[24] S.R. McKeown, P. Hatfield, R.J. Prestwich, R.E. Shaffer, R.E. Taylor, Radiotherapy for benign disease; assessing the risk of radiation-induced cancer following exposure to intermediate dose radiation, Br. J. Radiol. 88 (2015) 20150405.
[25] R. Ogawa, S. Akaishi, S. Kuribayashi, T. Miyashita, Keloids and hypertrophic scars can now be cured completely: recent progress in our understanding of the pathogenesis of keloids and hypertrophic scars and the most promising current therapeutic strategy, Journal of Nippon Medical School = Nippon Ika Daigaku Zasshi 83 (2016) 46–53.
[26] L. Rusciani, A. Paradisi, C. Alfano, S. Chiummariello, A. Rusciani, Cryotherapy in the treatment of keloids, Journal of Drugs in Dermatology: JDD 5 (2006) 591–595.
[27] E.E. Tredget, B. Nedelec, P.G. Scott, A. Ghahary, Hypertrophic scars, keloids, and contractures. The cellular and molecular basis for therapy, Surg. Clin. North Am. 77 (1997) 701–730.
[28] J.Q. Coentro, E. Pugliese, G. Hanley, M. Raghunath, D.I. Zeugolis, Current and upcoming therapies to modulate skin scarring and fibrosis, Adv. Drug Deliv. Rev. (2018), https://doi.org/10.1016/j.addr.2018.08.009.
[29] Z. Zhu, J. Ding, E.E. Tredget, The molecular basis of hypertrophic scars, Burns & Trauma 4 (2) (2016).
[30] P.H. Wang, B.S. Huang, H.C. Horng, C.C. Yeh, Y.J. Chen, Wound healing, Journal of the Chinese Medical Association: JCMA 81 (2018) 94–101.
[31] Z. Zhu, J. Ding, H.A. Shankowsky, E.E. Tredget, The molecular mechanism of hypertrophic scar, Journal of Cell Communication and Signaling 7 (2013) 239–252.
[32] J. Shi, Y. Wan, S. Shi, J. Zi, H. Guan, Y. Zhang, et al., Expression, purification, and characterization of scar tissue neovasculature endothelial cell-targeted rhIL10 in Escherichia coli, Appl. Biochem. Biotechnol. 175 (2015) 625–634.
[33] X. Wang, Z. Gao, X. Wu, W. Zhang, G. Zhou, W. Liu, Inhibitory effect of TGF-beta peptide antagonist on the fibrotic phenotype of human hypertrophic scar fibroblasts, Pharm. Biol. 54 (2016) 1189–1197.
[34] S. Garcia-Rates, P. Morrill, H. Tu, G. Pottiez, A.S. Badin, C. Tormo-Garcia, et al., (I) Pharmacological profiling of a novel modulator of the alpha7 nicotinic receptor: blockade of a toxic acetylcholinesterase-derived peptide increased in Alzheimer brains, Neuropharmacology 105 (2016) 487–499.
[35] K. Kanasaki, T. Nagai, K. Nitta, M. Kitada, D. Koya, N-acetyl-seryl-aspartyl-lysyl-proline: a valuable endogenous anti-fibrotic peptide

for combating kidney fibrosis in diabetes, Front. Pharmacol. 5 (2014) 70.
[36] L. Pickart, The human tri-peptide GHK and tissue remodeling, Journal of Biomaterials Science Polymer Edition 19 (2008) 969–988.
[37] T.A. Rohn, M. Boes, D. Wolters, S. Spindeldreher, B. Muller, H. Langen, et al., Upregulation of the CLIP self peptide on mature dendritic cells antagonizes T helper type 1 polarization, Nat. Immunol. 5 (2004) 909–918.
[38] K. Fosgerau, T. Hoffmann, Peptide therapeutics: current status and future directions, Drug Discov. Today 20 (2015) 122–128.
[39] P. Wang, L.Z. Jiang, B. Xue, Recombinant human endostatin reduces hypertrophic scar formation in rabbit ear model through down-regulation of VEGF and TIMP-1, Afr. Health Sci. 16 (2016) 542–553.
[40] A. Leask, D.J. Abraham, TGF-beta signaling and the fibrotic response, FASEB Journal: Official Publication of the Federation of American Societies for Experimental Biology 18 (2004) 816–827.
[41] J.W. Penn, A.O. Grobbelaar, K.J. Rolfe, The role of the TGF-beta family in wound healing, burns and scarring: a review, International Journal of Burns and Trauma 2 (2012) 18–28.
[42] I. Kashiwagi, R. Morita, T. Schichita, K. Komai, K. Saeki, M. Matsumoto, et al., Smad2 and Smad3 inversely regulate TGF-beta autoinduction in Clostridium butyricum-activated dendritic cells, Immunity 43 (2015) 65–79.
[43] H. Washio, N. Fukuda, H. Matsuda, H. Nagase, T. Watanabe, Y. Matsumoto, et al., Transcriptional inhibition of hypertrophic scars by a gene silencer, pyrrole-imidazole polyamide, targeting the TGF-beta1 promoter, The Journal of Investigative Dermatology 131 (2011) 1987–1995.